

# Compact Dual-Frequency Slot Antenna for C-Band Applications Based on Substrate Integrate Waveguide

Hussam Keriee<sup>1</sup>, Eman Hassan Essa<sup>1</sup>, Haider S. Mahdi<sup>2</sup>, Nawres Abbas Nayyef<sup>3</sup>

<sup>1</sup> Department of Medical Instrumentation Technical Engineering, Al-Hadi University College, Baghdad-10011, Iraq.

<sup>2</sup> Department of Medical Instrumentation Technical Engineering, College of Medical Techniques, Al-Farahidi University, Baghdad, Iraq.

<sup>3</sup> Faculty of Engineering & Technology, Multimedia University, Melaka, Malaysia.

---

## Article Info

### Article history:

Received Jun 2, 2023

Revised Dec 7, 2023

Accepted Dec 27, 2023

---

### Keywords:

Dual frequency,  
H-fractal slot,  
substrate integrated waveguide  
(SIW).

---

## ABSTRACT

This paper provides a compact substrate-integrated waveguide-based dual-frequency H-fractal slot antenna for the C-band (SIW). From the view of fractal slot antenna, two H-fractal slot shaped elements with 3rd iteration are used to cut currents in two TE modes, which leads to dual-frequency performance and reduces the size. The antenna operating at dual frequency of 4 GHz and 5.7 GHz with gain greater than 5 dB is designed and fabricated. Measured and simulated response of the antenna are introduced as well. The responses showed that the proposed antenna achieved stable dual-frequency performance with total size of  $23 \times 11$  mm<sup>2</sup>, which may be applied for C-band communication systems. The proposed antenna was simulated, analysed, and optimized using computer simulation technology (CST) software.

Copyright © 2023 Institute of Advanced Engineering and Science.  
All rights reserved.

---

## Corresponding Author:

Hussam Keriee

Department of Medical Instrumentation Technical Engineering, College of Medical Techniques, Al-Farahidi University, Baghdad, Iraq.

Email: sam22.utm@gmail.com

---

## 1. INTRODUCTION

The increasing needs for high gain antenna and compact size for industrial, scientific, and medical (ISM) communication system are outlined as a requirement for better wireless network performance[1]. Recently, Researchers are motivated to develop a high efficiency antenna by the rising need for multiple, dual, and wideband antennas. The primary objective is to boost data speeds using wideband antennas in order to increase traffic capacity at higher bands [2]. Besides, the trending between high performance antennas and its size should be taken in consideration at higher frequencies [3]. In general, standard planar transmission lines like microstrip were employed in the implementation of the antennas. However, there are a number of issues with the microstrip technology, including a high loss, undesirable crosstalk between lines, and difficulty fabricating in higher bands [4]. Additionally, low gain is another feature of Microstrip technology in higher bands. Substrate integrated waveguide (SIW) technology has so been suggested as a possible approach to implement the antenna.

Due to its low loss transmission line feature, (SIW) has recently been employed more frequently than conventional waveguide and microstrip technologies [5-10]. However, there are two significant difficulties with SIW antennas in lower millimeterwave bands. The substrate's vias (holes), which result in a larger size of antenna, are the first problem. The interior dimensions of the common waveguide determine the vias separation distance [11]. Additionally, these vias contain undesirable radiation losses that cause the antenna's gain to decrease and the sidelobes to rise [12-14]. The waveguide component of SIW presents the second challenge. The waveguide is widely recognized for having a narrow bandwidth [15, 16]. Thus, lower millimeterwave bands of SIW antenna may have a small bandwidth, This is not necessary for 5G applications or millimeterwave applications [17].

In the antenna systems and applications, the high quality of the antenna used is a major factor. The antenna should provide a multi-band and wideband reception points with high gain and high efficiency. Various types of antennas are proposed. However, these types suffered from low gain, and narrow bandwidth. Fractal antennas presents a good feature of repetitive, self-similar, and wideband. This is due to the main feature of the fractal antenna of procuring multi resonance frequencies. For example, a coplanar waveguide antenna in [18] is fed by triangular slot fractal shapes. The design obtained a high bandwidth of 8 GHz. Other types of fractal antennas can be seen [19]. The design in [19] is based on labyrinth fractal antenna. This achieved a high gain of 8 dB and bandwidth of 4 GHz. In [20] the antenna is based on conventional rectangular slot patch antenna. While in [21, 22], the antennas type is basically based on circular slot fractal shapes. Another fractal antenna also is presented in [23] which is designed with a finite ground co-planner waveguide (FG-CPW) circuit. The return losses are found better than 16 dB at 0.92 GHz and 2.45 GHz with fractional bandwidth of 3% at 10 dB return loss. In [23, 25], a fractal antenna is introduced. It is reported that the AR is 35% has been achieved. An efficiency is obtained at 2.45 GHz with 54%. Then the circuit is optimized to operate at frequency of 2.45 GHz. A 2.45 GHz circular polarization fractal antenna is designed and simulated using ADS software [26]. The design gives an AR of 65% and a return loss of -12 dB. An efficiency is obtained at 0.92 GHz and 2.45 GHz with 45% for each. Despite, the good performances of these antennas in capturing the waves from wide range of frequencies

Consequently, the purpose of this paper is to develop a small dual-band SIW antenna for the C-band. First, the design processes, such as fractal-shaped design and SIW antenna design, are covered in section 2. Second, section 3 shows the measured performance of the suggested SIW metamaterial antenna. In section 4, the summary of this work is completed.

## 2. DESIGN OF H-FRACTAL SLOT ANTENNA WITH SIW

Conventional SIW structure is shown in Figure 1. In SIW, The dielectric substrate has two rows of metallic vias that connect the parallel metal plates on the top and bottom and act as a waveguide. As well as the top and bottom metal plates, the two rows of vias act as the waveguide's walls. The basic structure is defined by its common parameters such as vias separation distance ( $w_{eff}$ ), vias diameter ( $d$ ), and the vias neighboring distance ( $p$ ). The separation distance ( $w_{eff}$ ) is depended on the waveguide inner size and dielectric properties. In general, other characteristics like substrate length, width, and high are determined using standard microstrip technology. The basic SIW parameters. The fractal slots are carved at waveguide centers, excited by the greatest electric field of the fundamental mode TE<sub>10</sub>, in order to produce high coupling between the SIW structures and the fractal slots. Three metamaterial unit cells and the typical SIW structure are shown together in Figure 2. The SIW structures-based metamaterial unit cells with the 1st, 2nd, and 3rd . H-shaped fractal slots are used in several iterations in order to maximize coupling and reduce the SIW structure size.

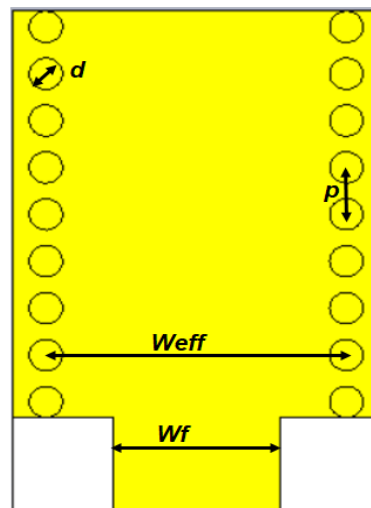


Figure 1. Conventional structure of SIW.

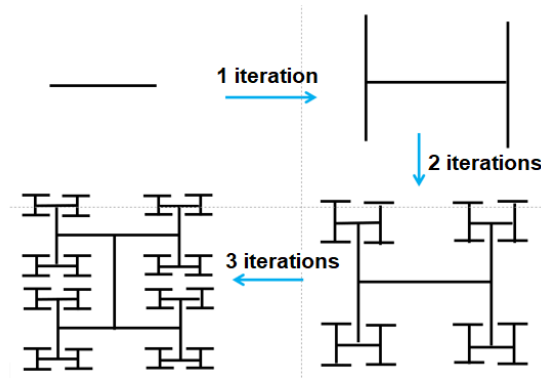


Figure 2. The proposed H-fractal shape with three iterations implemented on SIW.

The wide (top) walls of the SIW structures are above the H-fractal forms, as seen in Figure 3. However, slots can also be put in the SIW structures' foundations, producing roughly the same effects. In high-frequency radio systems, it is better to reduce noise and radiation losses while maintaining the stability of the construction. The suggested SIW-based H-fractal unit-cells and the conventional SIW's S-parameters research are shown in Figure 4. Considering each of the situations in Figure 3. Figure 4 shows that whereas conventional SIW forbids signals with evanescent modes below the cut-off frequency of the SIW structures of 10.3 GHz, the metamaterial unit cells enable signals under that cut-off frequency to flow through them. Thus, it can be defined as evanescent resonators.

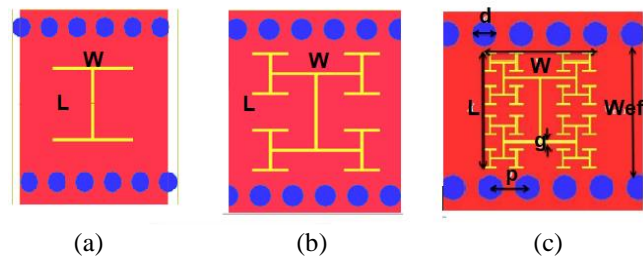


Figure 3. The proposed H-fractal shape unit cell on SIW structure. (a) 1st iteration, (b) 2nd iteration, (c) 3rd iteration.

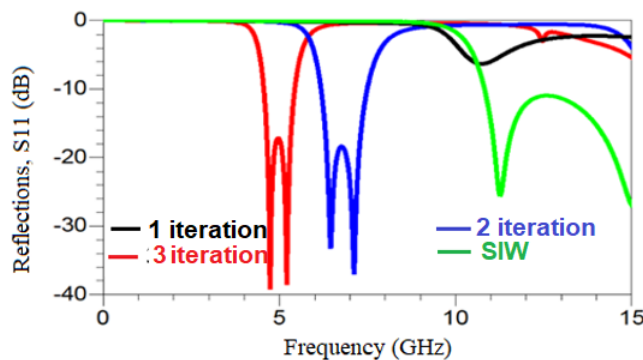


Figure 4. Simulated comparison between H-shaped fractal cells with SIW of input reflection (S11).

As 3rd iteration of H-fractal slot shape shifts the resonant frequency to lower band, the proposed SIW with 3rd iteration of H-shaped fractal cell is implement on SIW structure as shown in Figure 5. This allows a single frequency to be resonated. To study the effects of length (L) and width (W) of the H-fractal shape, a series of CST simulation are performed. By varying the length and the width of the H-shaped fractal antenna, the return loss increases and shifting to the desired frequency as shown in Figure 6.

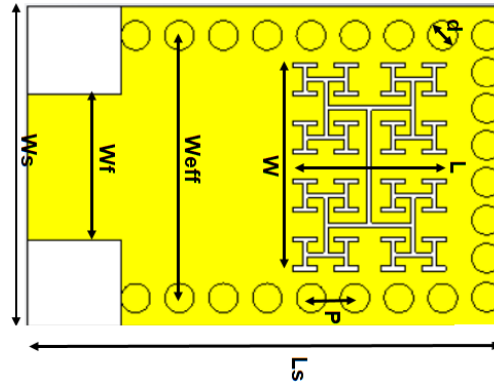


Figure 5. Structure of a closed-ended, single-element SIW antenna.

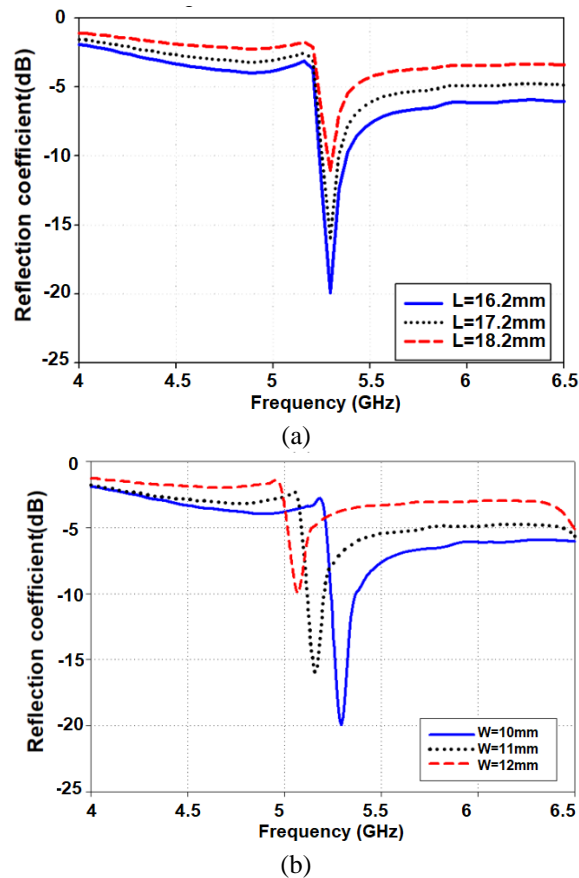


Figure 6. Reflection coefficient with different of SIW structure. (a) Different length, (b) different width.

Figure 7 shows an antenna configuration consisting of two elements H-shaped fractal of 3rd iteration to ensure two modes of resonant frequencies. The two adjusted H-shaped fractal are studied with different displacement ( $L_3$ ) to each other. Figure 8 shows the return loss with respect to different displacement ( $L_3$ ) between H-shaped fractal unit cells. It can be noticed that best response is obtained when width  $L_3 = 2.7$  mm. Two frequencies modes are observed in the targeted C-band at 4 GHz and 5.7 GHz. The final parameters of the proposed H-fractal shape SIW antenna for two frequency modes are depicted in Table 1. In addition, current surface distribution for the proposed antenna is shown in Figure 9. The two H-shaped fractal unit cells and the feed line are passed over by the current. Due to the altered structure of the cell unit, current flows in the opposite direction in each H-shaped fractal unit. The dual-mode frequency resonance is produced by the opposing current flowing through the two H-shaped fractal unit cells.

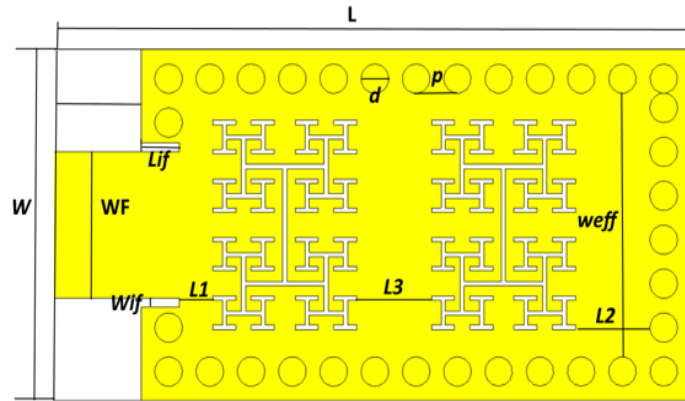


Figure 7. The proposed SIW antenna with two elements of 3rd iteration H-fractal shape unit.

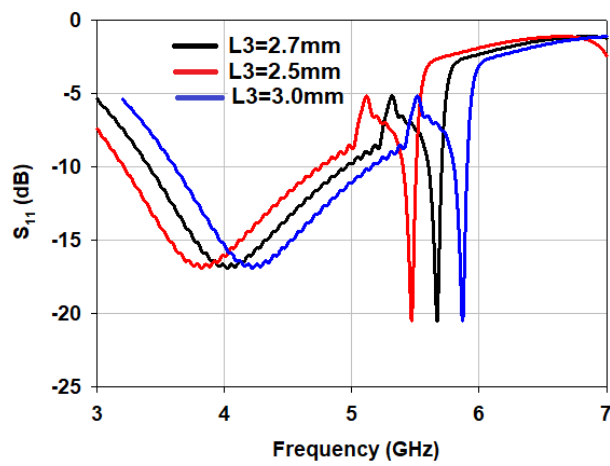


Figure 8. Return loss with different position of two adjusted H-fractal unit cell of SIW structure.

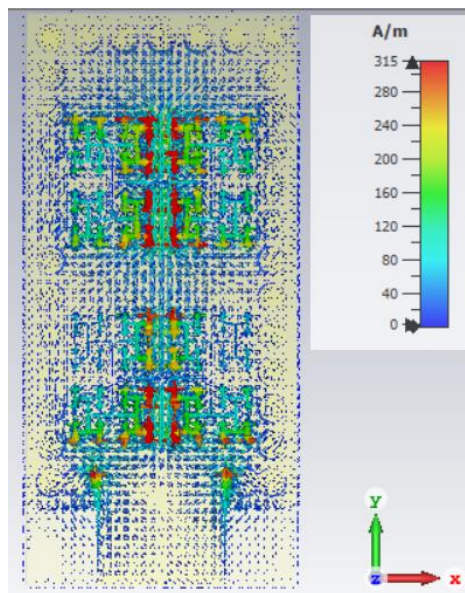


Figure 9. The current surface of the SIW H-fractal unit cell antenna at 4 and 5.7 GHz.

Table 1. SIW proposed antenna parameters.

Parameter	Value (mm)
L	23
W	11
$W_f$	5
d	0.5
p	1.5
$W_{eff}$	8
L1	1.21
L2	2.71
L3	2.7
f	4 GHz, 5.7 GHz

### 3. ANTENNA FABRICATION AND RESULTS

Figure 10 shows the picture of the fabricated H-shaped fractal SIW antenna with a total size of  $23 \times 11$  mm<sup>2</sup>. The measured reflection coefficient with respect to simulated one of the designed H-shaped metamaterial SIW antenna with short ended is shown in Figure 11. A reflection of -14.6 dB is obtained with bandwidth of 1.2 GHz at 4 GHz. Another frequency is resonated at 5.7 with a reflection of -17 dB and impedance bandwidth of 100 MHz, this is due to the two elements H-shaped unit cell of the SIW structure which allows to a second frequency to be resonated.

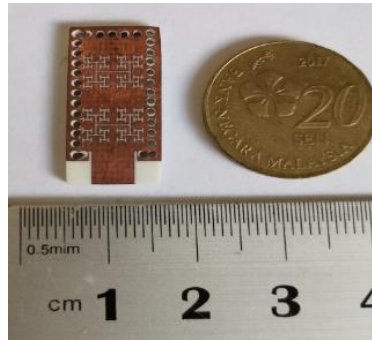


Figure 10. Fabricated H-shaped fractal SIW antenna.

Figure 12 shows the measured radiation pattern with respected with simulated radiation of the printed SIW H-shaped antenna at 4 GHz and 5.7 GHz. The radiation pattern of omni-directional shape is observed with sidelobes less than -10 dB. In that term directivity of the printed antenna are 5 dB and 3 dB at 4 GHz and 5.7 GHz respectively. Table 2 shows a comparison between this SIW dual H-shaped unit cell antennas with other related works. This antenna exploited a good bandwidth and compact size of  $23 \text{ mm} \times 11 \text{ mm}$  among others with total reduction in size of 20%.

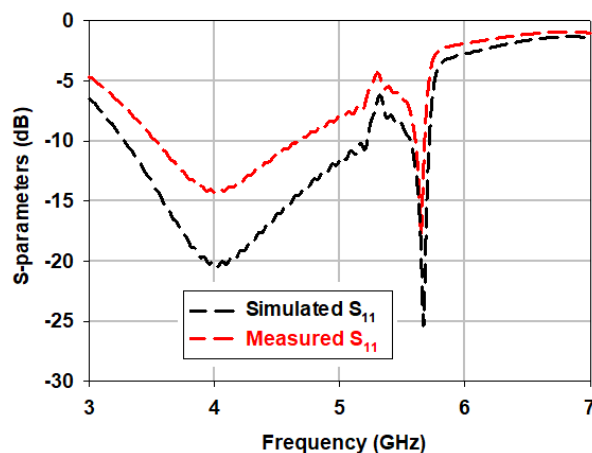


Figure 11. The measured and simulated reflection coefficient (S11) of antenna.

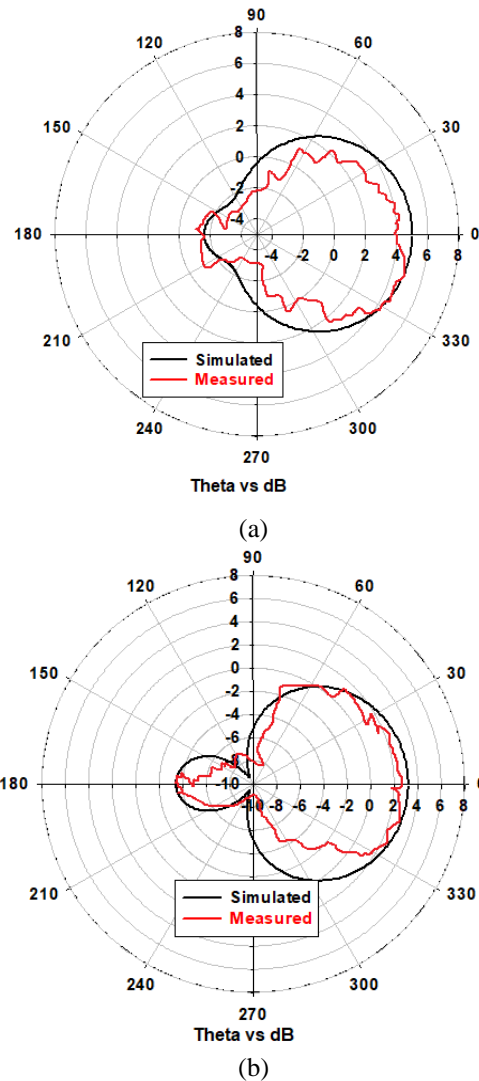


Figure 12. The SIW dual H-shaped antenna with short end's measured radiation pattern. (a) radiation at 4 GHz, (b) radiation at 5.7 GHz.

Table 2. Comparison of antenna with other works.

Parameters/ref	[9]	[10]	[12]	This work
Frequency (GHz)	8.26	5.83	10	4, 5.7
S11 (dB)	-20	-13	-20	-14, -17
Bandwidth (GHz)	0.5	0.45	1.5	1.2
Gain (dB)	3.56	12	4.9	5, 3
Size (mm <sup>2</sup> )	23 × 32	174 × 109	29 × 23	23 × 11

#### 4. CONCLUSION

In this paper, a portable dual-band SIW antenna for the C-band was introduced. H-fractal slot cell technology combined with a SIW structure is used to implement the design. Two elements of 3rd H-shaped fractal unit cell are used to control the bandwidth and achieved the dual-band property. Good results are obtained with reflection coefficient less than 10 dB at 4 GHz and 5.7 GHz. A gain of 5 dB is achieved at 4 GHz with high efficiency of 80 %. 1.2 GHz wideband impedance is also observed at the same time. This antenna provides a feasible method for assembling the best possible array of antennas, which would be useful for current wireless and lower millimeterwave applications.

#### REFERENCES

- [1] H. H. Keriee et al., "High gain antenna at 915 MHz for off grid wireless networks," Bulletin of Electrical Engineering and Informatics, vol. 9, no. 6, pp. 2449-2454, 2020.
- [2] T. Li and Z. N. Chen, "Wideband substrate-integrated waveguide-fed end fire meta surface antenna array," IEEE Transactions on Antennas and Propagation, vol. 66, pp. 7032-7040, 2018.

- [3] P. N. Choubey, W. Hong, Z.-C. Hao, P. Chen, T.-V. Duong, and J. Mei, "A wideband dual-mode SIW cavity-backed triangular-complimentary-split-ring-slot (TCSRS) antenna," *IEEE Transactions on Antennas and propagation*, vol. 64, pp. 2541-2545, 2016..
- [4] K. Pedram, J. Nourinia, C. Ghobadi, N. Pouyanfar, and M. Karamirad, "Compact and miniaturized metamaterial-based microstrip fractal antenna with reconfigurable qualification," *AEU-International Journal of Electronics and Communications*, vol. 114, p. 152959, 2020.
- [5] W. Wahba, M. A. Abdalla, and A. M. Allam, "Experimental verification of a compact zeroth order metamaterial substrate integrated waveguide antenna," *Progress In Electromagnetics Research*, vol. 67, pp. 193-201, 2016.
- [6] S. Choudhury and A. Mohan, "Miniaturized Sierpinski fractal loaded QMSIW antenna with CSRR in ground plane for WLAN applications," *Microwave and Optical Technology Letters*, vol. 59, pp. 1291-1295, 2017.
- [7] M. Adhikary, S. K. Sahoo, A. Biswas, and M. J. Akhtar, "SIW-Based Self-Oscillating Concurrent Dual-Frequency Active Integrated Antenna," *IEEE Antennas and Wireless Propagation Letters*, vol. 18, pp. 1897-1901, 2019.
- [8] M. Danaeian, K. Afrooz, and A. Hakimi, "Miniaturization of substrate integrated waveguide filters using novel compact metamaterial unit-cells based on SIR technique," *AEU-International Journal of Electronics and Communications*, vol. 84, pp. 62-73, 2018.
- [9] R. Agrawal, P. Belwal, and S. Gupta, "Half Mode Substrate Integrated Waveguide Leaky Wave Antenna with Broadside Gain Enhancement for Ku-Band Applications," *Radioengineering*, vol. 28, pp. 565-571, 2019.
- [10] L. Wang, J. L. Gómez-Tornero, and O. Quevedo-Teruel, "Substrate integrated waveguide leaky-wave antenna with wide bandwidth via prism coupling," *IEEE transactions on microwave theory and techniques*, vol. 66, pp. 3110-3118, 2018.
- [11] S. S. Hesari and J. Bornemann, "Wideband circularly polarized substrate integrated waveguide endfire antenna system with high gain," *IEEE Antennas and Wireless Propagation Letters*, vol. 16, pp. 2262-2265, 2017.
- [12] M. M. Honari, R. Mirzavand, H. Saghlatoon, and P. Mousavi, "A dual-band low-profile aperture antenna with substrate-integrated waveguide grooves," *IEEE Transactions on Antennas and Propagation*, vol. 64, pp. 1561-1566, 2016.
- [13] B.-J. Niu, J.-H. Tan, and C.-L. He, "SIW cavity-backed dual-band antenna with good stopband characteristics," *Electronics Letters*, vol. 54, pp. 1259-1260, 2018.
- [14] Y. Shi, J. Liu, and Y. Long, "Wideband triple-and quad-resonance substrate integrated waveguide cavity-backed slot antennas with shorting vias," *IEEE Transactions on Antennas and Propagation*, vol. 65, pp. 5768-5775, 2017.
- [15] H. Lee, D. Ren, and J. H. Choi, "Dual-band and polarization-flexible CRLH substrate-integrated waveguide resonant antenna," *IEEE Antennas and Wireless Propagation Letters*, vol. 17, pp. 1469-1472, 2018.
- [16] Z. Fu, T. Zhang, Y. Lan, T. Wu, W. Huang, and L. He, "Dual-Frequency Miniaturized Substrate Integrated Waveguide Quarter-Mode Cavity-Backed Antenna Based on Minkowski Fractal Gap with Orthogonal Polarization Radiation Characteristics," *International Journal of Antennas and Propagation*, vol. 2019, 2019.
- [17] S. Schulz, M. Becker, M. R. Groseclose, S. Schadt, and C. Hopf, "Advanced MALDI mass spectrometry imaging in pharmaceutical research and drug development," *Curr. Opin. Biotechnol.*, vol. 55, pp. 51-59, 2019, doi: 10.1016/j.copbio.2018.08.003.
- [18] N. Rao, "Modified Sierpinski and its use in Fractal Patch Antenna for Miniaturization and Multiband Behavior," *2022 IEEE Microwaves, Antennas, and Propagation Conference (MAPCON)*, Bangalore, India, 2022, pp. 1804-1809.
- [19] S. Shankar and D. K. Upadhyay, "A Fractal Monopole Antenna With Dual Polarization Reconfigurable Characteristics for X-Band Applications," in *IEEE Access*, vol. 11, pp. 95667-95680, 2023.
- [20] Y. Kumar, R. K. Gangwar and B. K. Kanaujia, "Characterization of CP Radiations in a Planar Monopole Antenna Using Tuning Fork Fractal Slot for LTE Band13/Wi-Max and Wi-Fi Applications," in *IEEE Access*, vol. 8, pp. 127123-127133, 2020.
- [21] B. Karibayev, N. Meirambekuly, T. Namazbayev, B. Kozhakhmetova, K. Chizhimbayeva and A. Kulakayeva, "The Possibilities of Using Fractal Antennas in Modern Wireless Communication Technologies," *2023 IEEE International Conference on Smart Information Systems and Technologies (SIST)*, Astana, Kazakhstan, 2023, pp. 184-188.
- [22] F. Lihua and Bijiaming, "Design and Optimization of Plane Microstrip Fractal Antenna Based on Y Structure," *2020 IEEE MTT-S International Microwave Workshop Series on Advanced Materials and Processes for RF and THz Applications (IMWS-AMP)*, Suzhou, China, 2020, pp. 1-3.
- [23] M. Sreenivasulu, E. K. Kumari, R. R. Reddy and S. B. T. Abhyuday, "Minkowski Fractal Antenna with Circular DGS for Multiband Applications," *2022 IEEE Wireless Antenna and Microwave Symposium (WAMS)*, Rourkela, India, 2022, pp. 1-5.
- [24] H. Yang and W. Yang, "An Ultra-Wideband Microstrip Antenna Based on Koch Fractal Resonance Unit and CSRRs Defective Ground Unit," *2020 9th Asia-Pacific Conference on Antennas and Propagation (APCAP)*, Xiamen, China, 2020, pp. 1-2.
- [25] M. Y. I. Yazid, M. H. Baharuddin, M. S. Islam, M. T. Islam and A. F. Almutairi, "A Sierpinski Arrowhead Curve Slot Vivaldi Antenna for Microwave Head Imaging System," in *IEEE Access*, vol. 11, pp. 32335-32347, 2023.
- [26] . Ez-Zaki *et al.*, "Double Negative (DNG) Metamaterial-Based Koch Fractal MIMO Antenna Design for Sub-6-GHz V2X Communication," in *IEEE Access*, vol. 11, pp. 77620-77635, 2023.